A novel widespread bacterial structure related to the flagellar type III secretion system

Mohammed Kaplan[1], Catherine M Oikonomou[1], Cecily R. Wood[2], Georges Chreifi[1], Debnath Ghosal[3], Megan J Dobro[4], Qing Yao[1], Alasdair McDowall[1], Ariane Briegel[5], Morgan Beeby[6], Yi-Wei Chang[7], Carrie L. Shaffer[2,8,9], Grant J. Jensen[1,10,11]

Affiliations

[1]Division of Biology and Biological Engineering, California Institute of Technology, Pasadena, CA 91125, USA

[2]University of Kentucky Department of Veterinary Science

[3]Division of Medicine, Dentistry and Health Sciences, University of Melbourne, Parkville, Victoria, Australia

[4]Hampshire College, Amherst, Massachusetts, USA

[5]Leiden University, Sylvius Laboratories, Leiden, The Netherlands

[6]Department of Life Sciences, Imperial College London, South Kensington Campus, London SW7 2AZ, UK

[7]Department of Biochemistry and Biophysics, Perelman School of Medicine, University of Pennsylvania, Philadelphia, PA 19104, USA

[8]University of Kentucky Department of Microbiology, Immunology, and Molecular Genetics

[9]University of Kentucky Department of Pharmaceutical Sciences

[10]Department of Chemistry and Biochemistry, Brigham Young University, Provo, UT 84604, USA

[11]Corresponding author: jensen@caltech.edu

Abstract

The flagellar type III secretion system (fT3SS) is a suite of membrane-embedded and cytoplasmic proteins responsible for building the bacterial flagellar motility machinery. Homologous proteins form the injectisome machinery bacteria use to deliver effector proteins into eukaryotic cells, and other family members have recently been reported to be involved in the formation of membrane nanotubes. Here we describe a novel, ubiquitous and evolutionarily widespread hat-shaped structure embedded in the inner membrane of bacteria, of yet-unidentified function, that is related to the fT3SS, adding to the already rich repertoire of this family of nanomachines.

Type III secretion systems (T3SS) assemble bacterial machinery with diverse functions. In addition to forming the flagellum and the injectisome, they have also been reported recently to be involved in the formation of membrane tubes [1]. The flagellar type III secretion system (fT3SS) consists of a cytoplasmic part containing an ATPase and an inner-membrane (IM)-embedded part known as the core complex (fT3SScc). The fT3SScc consists of five proteins (FliP, FliQ, FliR, FlhB and FlhA), with another protein, FliO, required for assembly but which does not form part of the complex [2,3]. Initially, FliP forms a pentameric platform on which FliQ, FliR and FlhB assemble to create a $FliP_5FliQ_4FliR_1FlhB_1$ subcomplex upon which an FlhA ring is built [4].

While using electron cryo-tomography (cryo-ET) to study the process of flagellar assembly in *Helicobacter pylori*, we identified a periplasmic hat-shaped structure embedded in the inner membrane (IM) of the cell (Fig. 1). The structure was abundant and, in contrast to the polar flagella of this species, did not show any preferred spatial localization in the cell (e.g., not exclusively at the cell pole). Carefully reexamining tens of thousands of cryotomograms of other, phylogenetically-diverse bacterial species our lab has imaged over the past 15 years, we found that this hat-like structure is widespread in diverse Gram-negative and Gram-positive bacteria (Fig. 2; see also Supporting Figure S1). In many cases, we observed multiple hat-like structures (up to 10 in some cells) distributed around the cell (see Movie S1 for an example from an *E. coli* cell that was partially lysed, enhancing visibility of periplasmic structures). Subtomogram averages of the structure from different species revealed conserved characteristics: a hat-shaped part in the periplasm and two cytoplasmic densities beneath (Fig. 2). In general, the periplasmic hat-like portion had a diameter of ~24-26 nm at its widest point at the outer surface of the IM. The cytoplasmic densities were absent in the averages from three species: *Pseudoalteromonas*

luteoviolacea, *Hylemonella gracilis* and *Bacillus subtilis*. The absence of these densities in *P. luteoviolacea* and *B. subtilis* is likely due to the fact that these were lysed and not intact cells. We also observed that the cytoplasmic density did not resolve into two distinct sections in all species.

We also identified the same structure in several *H. pylori* flagellar mutants: *fliP*,* Δ*flgS fliP**, Δ*fliM fliP**, Δ*fliG fliP**, Δ*fliO fliP*,* and Δ*fliQ fliP**. The *H. pylori fliP** strain contains a naturally-occurring point mutation that disrupts the function of FliP [5] and prevents the assembly of the fT3SScc (manuscript in preparation). The other mutants remove additional fT3SScc proteins (Δ*fliO* and Δ*fliQ*), flagellar basal body proteins (Δ*fliM* and Δ*fliG*), or the tyrosine kinase responsible for expression of the class II flagellar genes (Δ*flgS*) [6]. Curiously, in all of these mutants the diameter of the hat-like density was reduced to only ~20 nm (at its widest part) and the two cytoplasmic densities were missing (or less well resolved) (Fig. 3 A-G). This difference was not due to decreased resolution, since more particles were averaged than from wild-type cells (see Materials and Methods). This observation suggested to us that the hat-like structure is related to the fT3SScc. Indeed the general shape is reminiscent of the MS-ring of the flagellar motor, and we observed the disappearance of two similar cytoplasmic densities in the motor (corresponding to $FlhA_C$) in the same mutants while studying flagellar assembly (manuscript in preparation). The reduced width of the hat-like structure in *fliP** cells is also reminiscent of the reduced width of flagellar complexes in the absence of the fT3SScc [7].

To explore this relationship, we examined *Campylobacter jejuni* mutants of other fTSScc proteins. These included mutants of the C-terminal domains of FlhA (Δ*flhAc*) and FlhB (Δ*flhBc*) [8]. In Δ*flhAc* cells, compared to wild-type, the periplasmic hat-like part was again smaller in diameter

and the two cytoplasmic densities disappeared (Fig. 3 I & J). In contrast, the hat-like structure in Δ*flhBc* cells was indistinguishable from the wild-type complex both in diameter and the presence of the associated cytoplasmic densities (Fig. 3 K). This is not too surprising, since, unlike the large pentameric FliP ring or the nonameric FlhA ring, FlhB is a small protein present in a monomeric form in the fT3SScc. Although the absence of the C-terminus of FlhB renders the fT3SS non-functional (no full flagella assemble in Δ*flhBc C. jejuni* [8]), the fT3SScc can still assemble (manuscript in preparation). To confirm the generality of the relationship between the fT3SScc and the hat-like complex, we imaged an *flhA* mutant in *P. aeruginosa* (*flhA**, obtained from a transposon insertion mutant library). Here also, the hat-like structure was smaller in size and lacked clear cytoplasmic densities compared to wild-type (Fig. 3 L & M).

Based on the apparent relationship between the fT3SScc and the hat-like structure, we hypothesized that the novel complex is formed by the flagellar MS-ring protein, FliF, adopting a different, more closed conformation than that seen in the fully-assembled flagellar motor. Hence, we generated and imaged a Δ*fliF* mutant in the *H. pylori fliP** background. However, the hat-like complex was still present in this mutant, indicating that it is not formed by FliF (Fig. 3 H). Thus our observations suggest that while the cytoplasmic densities of the complex could be $FlhA_C$, the periplasmic density is not formed by FliF or any of the fT3SScc proteins. Of course, it is also possible that $FlhA_C$ does not directly constitute the cytoplasmic densities, but rather that the fT3SScc proteins are regulating the expression (or localization) of another protein(s) that does.

One possibility is that the hat-like structure we discovered here might represent an as-yet unidentified scaffold that helps the fT3SScc assemble. If this structure is some sort of scaffold and

105 the fT3SScc (or part of it) assembles within the hat-like portion and if the cytoplasmic densities
106 are $FlhA_C$, this would explain the disappearance of the cytoplasmic densities and the smaller
107 diameter of the periplasmic portion in *fliP** and *flhA* mutants. The second possibility is that
108 fT3SScc proteins in some way regulate other proteins which themselves form the hat-like complex.
109 Such a regulatory role has been indicated previously for one of the fT3SScc proteins, FliO, which
110 is responsible for the optimal expression of other flagellar genes [9].
111
112 Whatever the function of this hat-like complex, it joins the already-rich repertoire of the (f)T3SS,
113 which has roles in flagellar motility, protein translocation and possibly membrane nanotube
114 formation. Whether the hat-like structure is connected to any of these functions or plays another,
115 yet-unidentified role remains to be elucidated. It is also possible that the apparently ancient
116 structure may have diverged to serve different functions in different species.
117

References:

1. Bhattacharya S, Baidya AK, Pal RR, Mamou G, Gatt YE, Margalit H, et al. A Ubiquitous Platform for Bacterial Nanotube Biogenesis. Cell Reports. 2019;27: 334-342.e10. doi:10.1016/j.celrep.2019.02.055

2. Fabiani FD, Renault TT, Peters B, Dietsche T, Gálvez EJC, Guse A, et al. A flagellum-specific chaperone facilitates assembly of the core type III export apparatus of the bacterial flagellum. Stock A, editor. PLOS Biology. 2017;15: e2002267. doi:10.1371/journal.pbio.2002267

3. Fukumura T, Makino F, Dietsche T, Kinoshita M, Kato T, Wagner S, et al. Assembly and stoichiometry of the core structure of the bacterial flagellar type III export gate complex. Stock A, editor. PLOS Biology. 2017;15: e2002281. doi:10.1371/journal.pbio.2002281

4. Milne-Davies B, Wimmi S, Diepold A. Adaptivity and dynamics in type III secretion systems. Mol Microbiol. 2021;115: 395–411. doi:10.1111/mmi.14658

5. Chang Y-W, Shaffer CL, Rettberg LA, Ghosal D, Jensen GJ. In Vivo Structures of the Helicobacter pylori cag Type IV Secretion System. Cell Reports. 2018;23: 673–681. doi:10.1016/j.celrep.2018.03.085

6. Lertsethtakarn P, Ottemann KM, Hendrixson DR. Motility and Chemotaxis in *Campylobacter* and *Helicobacter*. Annual Review of Microbiology. 2011;65: 389–410. doi:10.1146/annurev-micro-090110-102908

7. Johnson S, Fong YH, Deme JC, Furlong EJ, Kuhlen L, Lea SM. Symmetry mismatch in the MS-ring of the bacterial flagellar rotor explains the structural coordination of secretion and rotation. Nature Microbiology. 2020 [cited 3 May 2020]. doi:10.1038/s41564-020-0703-3

8. Abrusci P, Vergara-Irigaray M, Johnson S, Beeby MD, Hendrixson DR, Roversi P, et al. Architecture of the major component of the type III secretion system export apparatus. Nature Structural & Molecular Biology. 2013;20: 99–104. doi:10.1038/nsmb.2452

9. Tsang J, Hoover TR. Requirement of the Flagellar Protein Export Apparatus Component FliO for Optimal Expression of Flagellar Genes in Helicobacter pylori. Journal of Bacteriology. 2014;196: 2709–2717. doi:10.1128/JB.01332-13

151 **Figures**

152 **Figure 1**

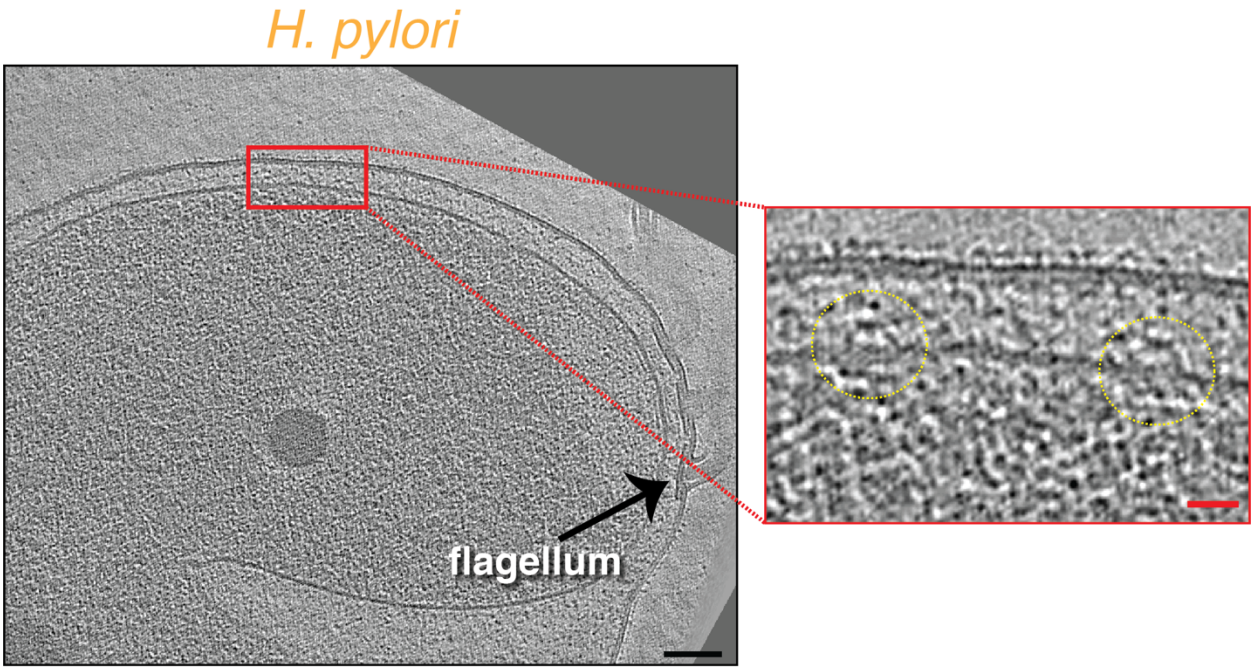

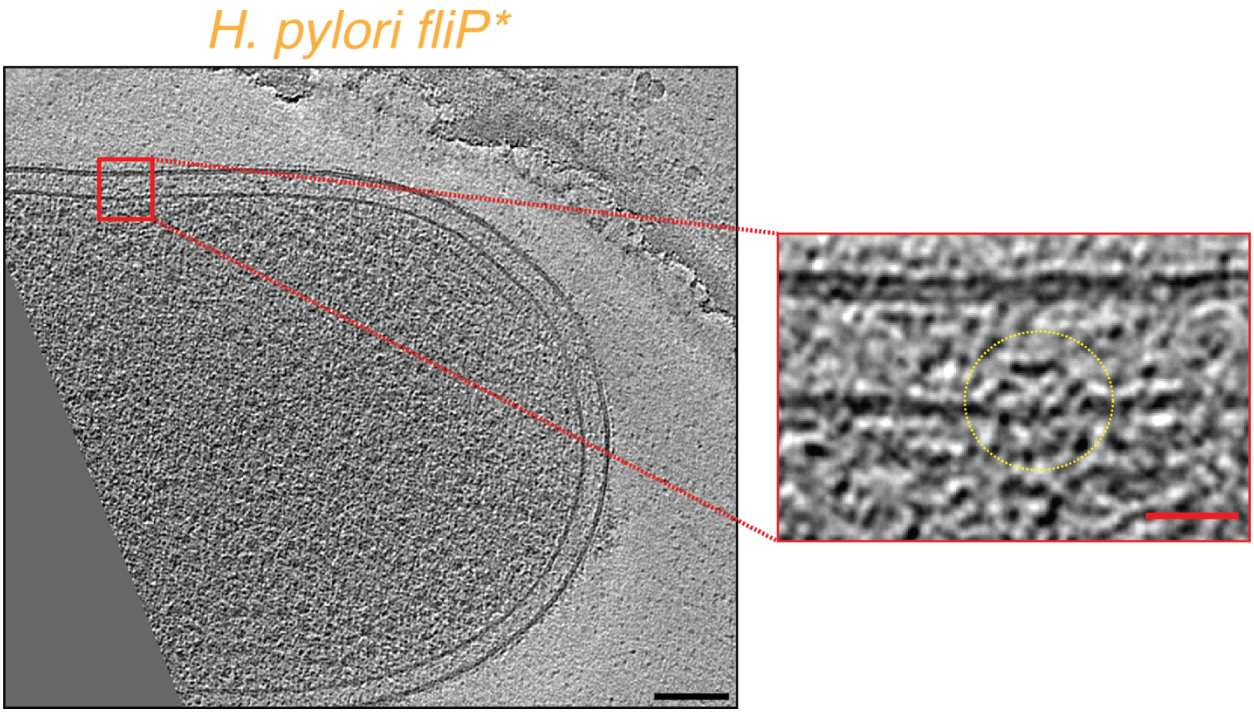

153

154

Figure 2

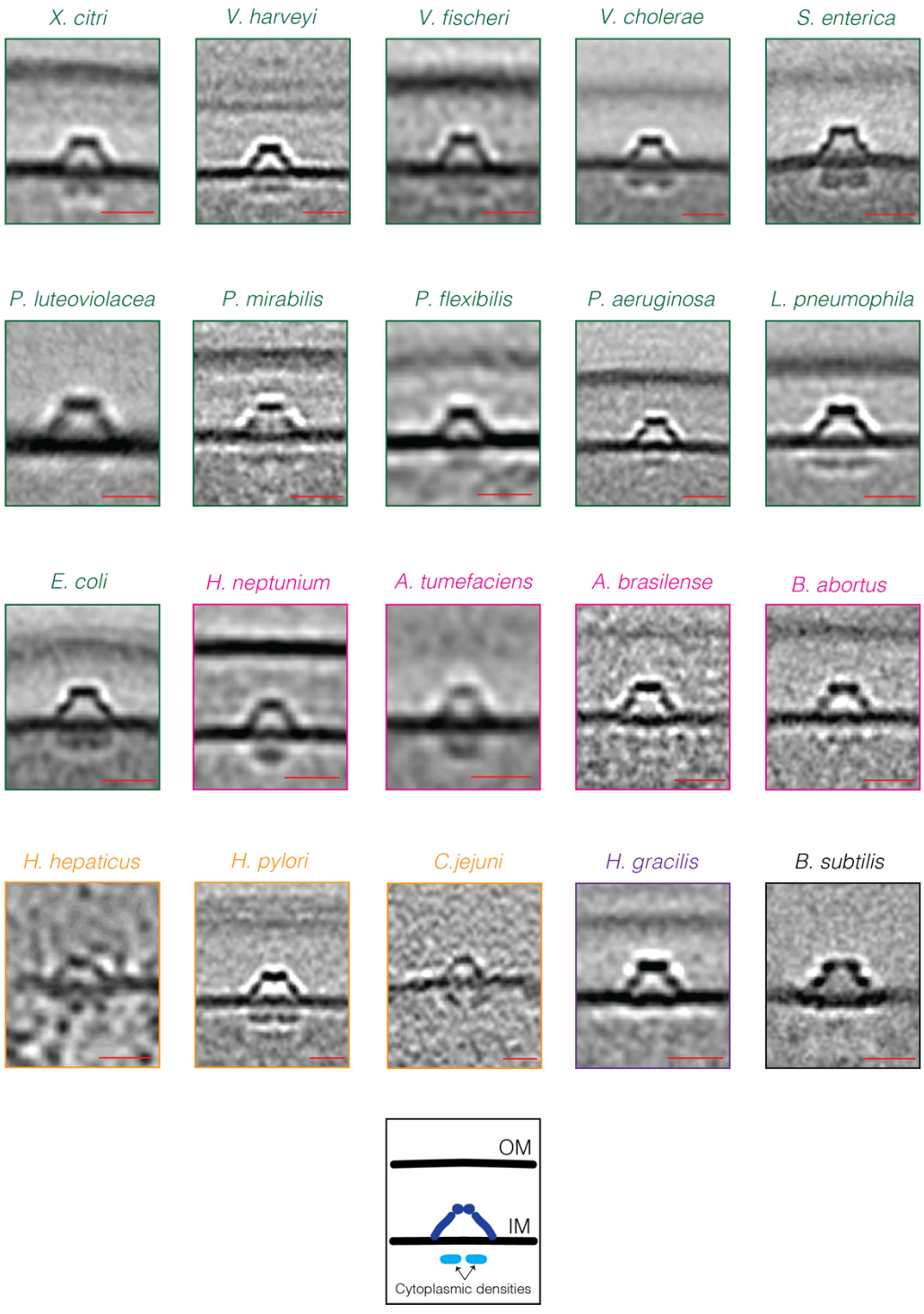

177 **Figure 3**

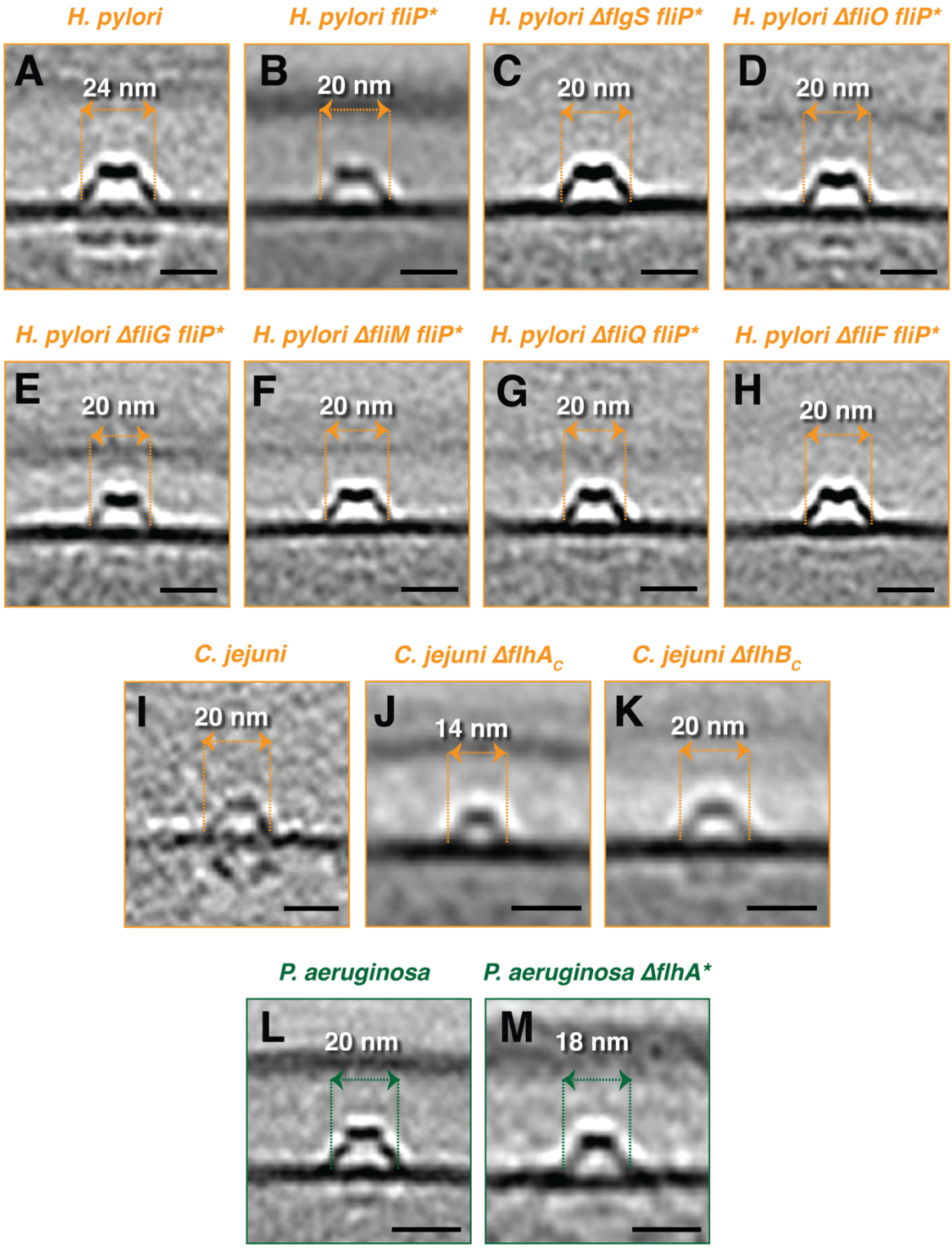

178

179

Figure legends:

Figure 1: Identification of a novel hat-like complex in *H. pylori*. A & B) slices through electron cryotomograms of *H. pylori* (A) or *H. pylori fliP** (B) cells showing the presence of hat-like complexes (enlarged in red boxes). Black scale bars 100 nm, red scale bars 25 nm.

Figure 2: The hat-like complex is a widespread bacterial structure. A gallery of the hat-like complex in different bacterial species (*Xanthomonas citri*, *Vibrio harveyi*, *V. fischeri*, *V. cholerae*, *Salmonella enterica*, *Pseudoalteromonas luteoviolacea*, *Proteus mirabilis*, *Pseudomonas flexibilis*, *P. aeruginosa*, *Legionella pneumophila*, *Escherichia coli*, *Hyphomonas neptunium*, *Agrobacterium tumefaciens*, *Azospirillum brasilense*, *Brucella abortus*, *Helicobacter hepaticus*, *H. pylori*, *Campylobacter jejuni*, *Hylemonella gracilis* and *Bacillus subtilis*). Sub-tomogram averages are shown, except for *C. jejuni* and *H. hepaticus,* where not enough data was available for averaging so single tomographic slices are shown. Color coding indicates taxonomic class: green, Gammaproteobacteria; pink, Alphaproteobacteria; yellow, Epsilonproteobacteria; purple, Betaproteobacteria; and black, Bacilli. Scale bars are 20 nm.

Figure 3: The effect of various flagellar-related mutations on the hat-like complex. Central slices through sub-tomogram averages (except (I), where a single tomographic slice is shown) of the hat-like complex in wild-type cells and the indicated mutants of *H. pylori* **(A-H)**, *C. jejuni* **(I-K)** and *P. aeruginosa* **(L & M)**. Scale bars are 20 nm.

Supporting Information for

A novel widespread bacterial structure related to the flagellar type III secretion system

Mohammed Kaplan[1], Catherine M Oikonomou[1], Cecily R. Wood[2], Georges Chreifi[1], Debnath Ghosal[3], Megan J Dobro[4], Qing Yao[1], Alasdair McDowall[1], Ariane Briegel[5], Morgan Beeby[6], Yi-Wei Chang[7], Carrie L. Shaffer[2,8,9], Grant J. Jensen[1,10,11]

209 **Supporting Figures:**

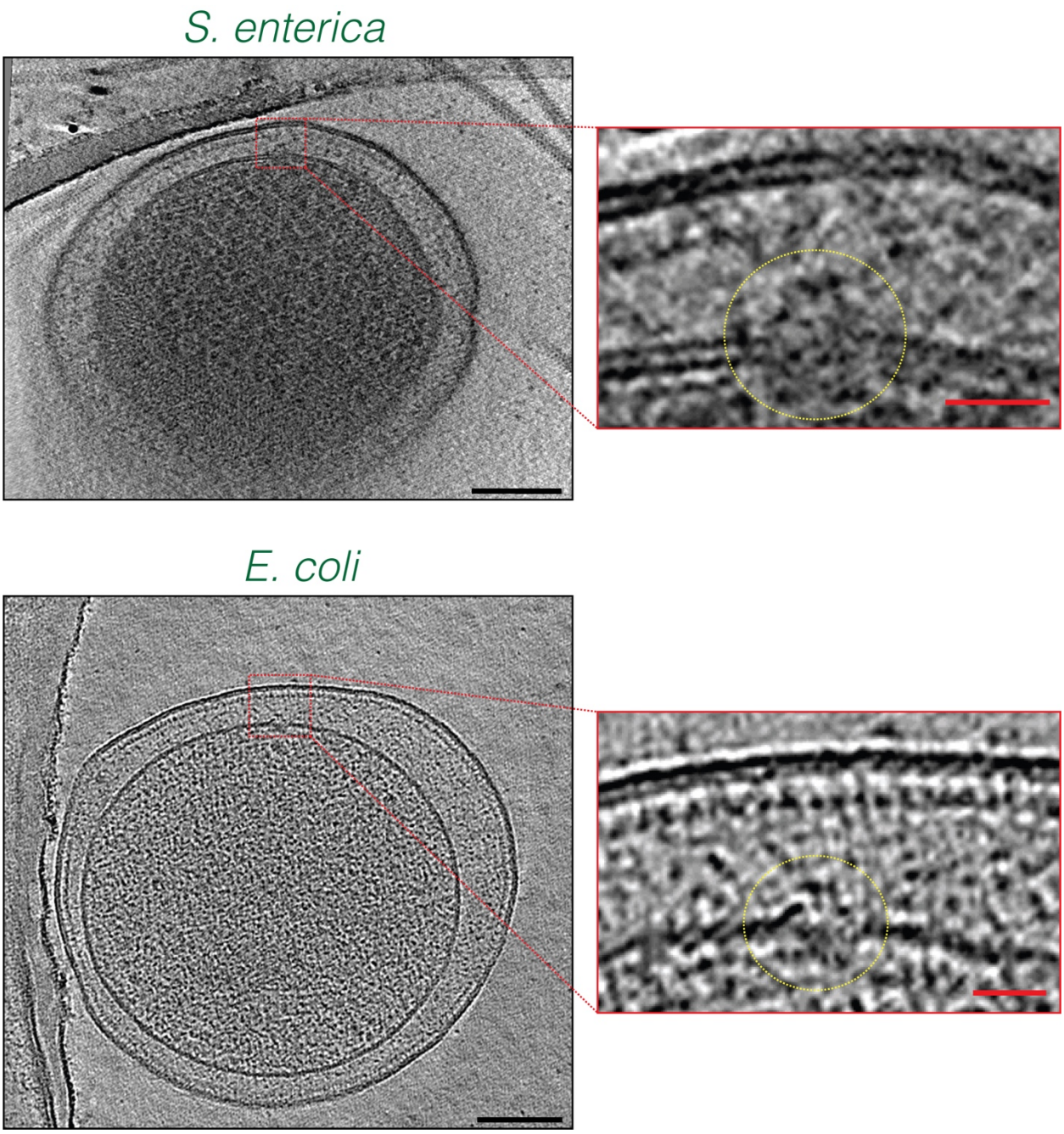

210

211

212

213

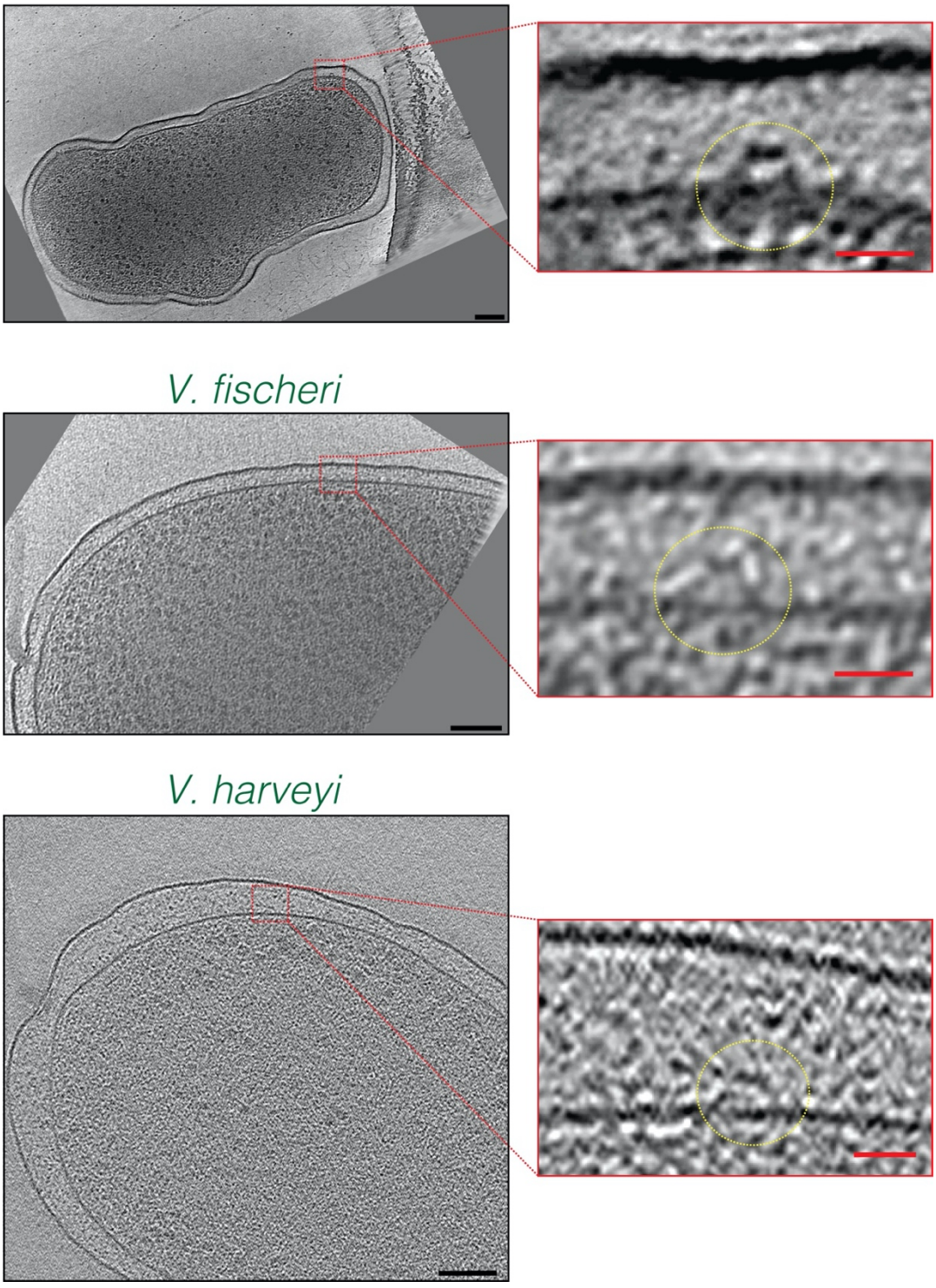

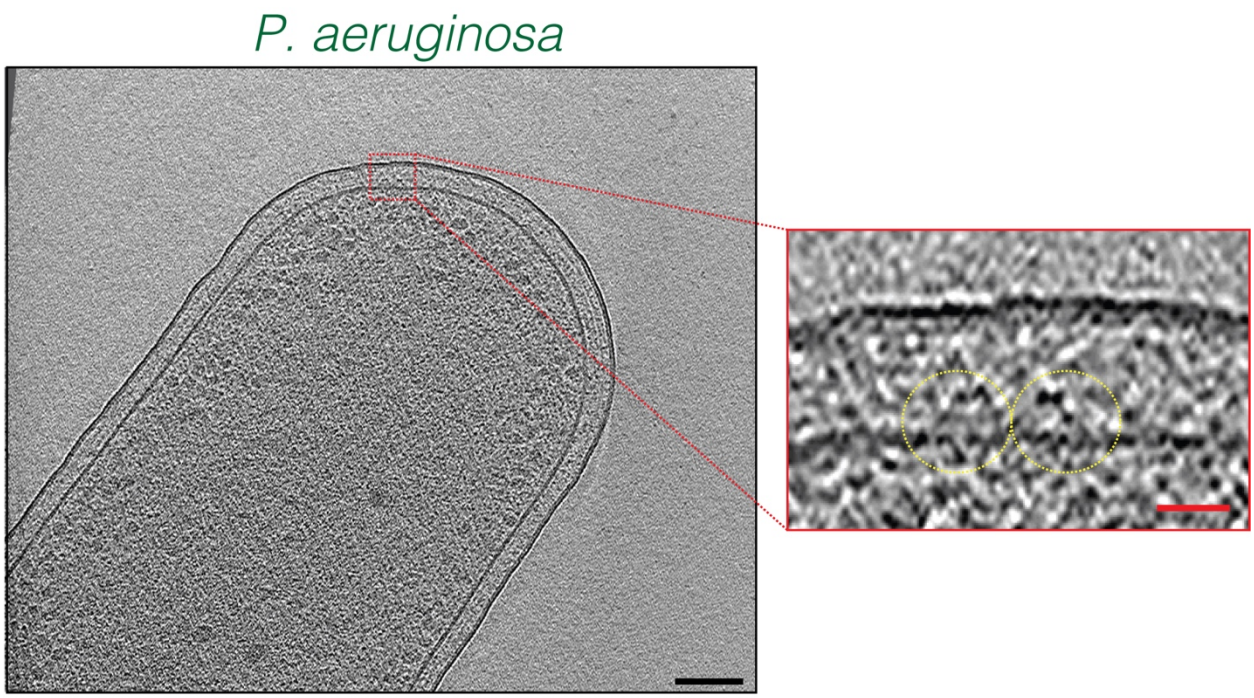

237

238

239

240

241

242

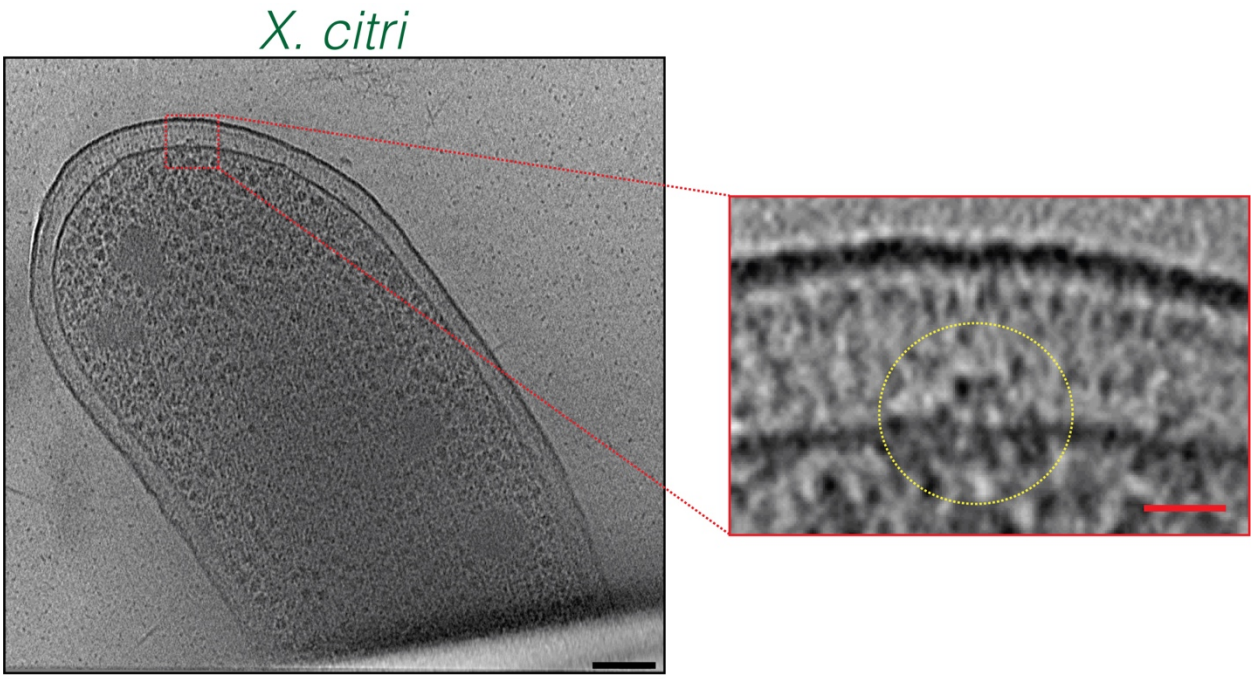

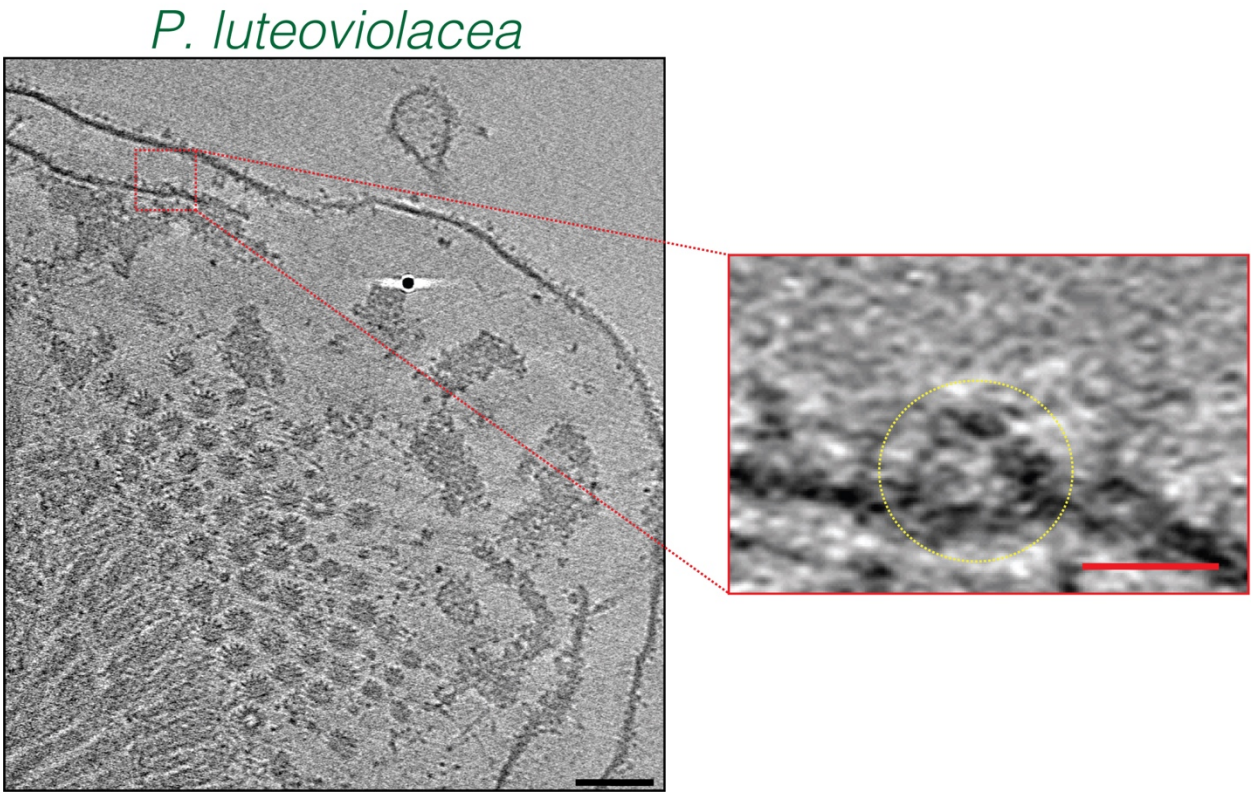

243

244

245

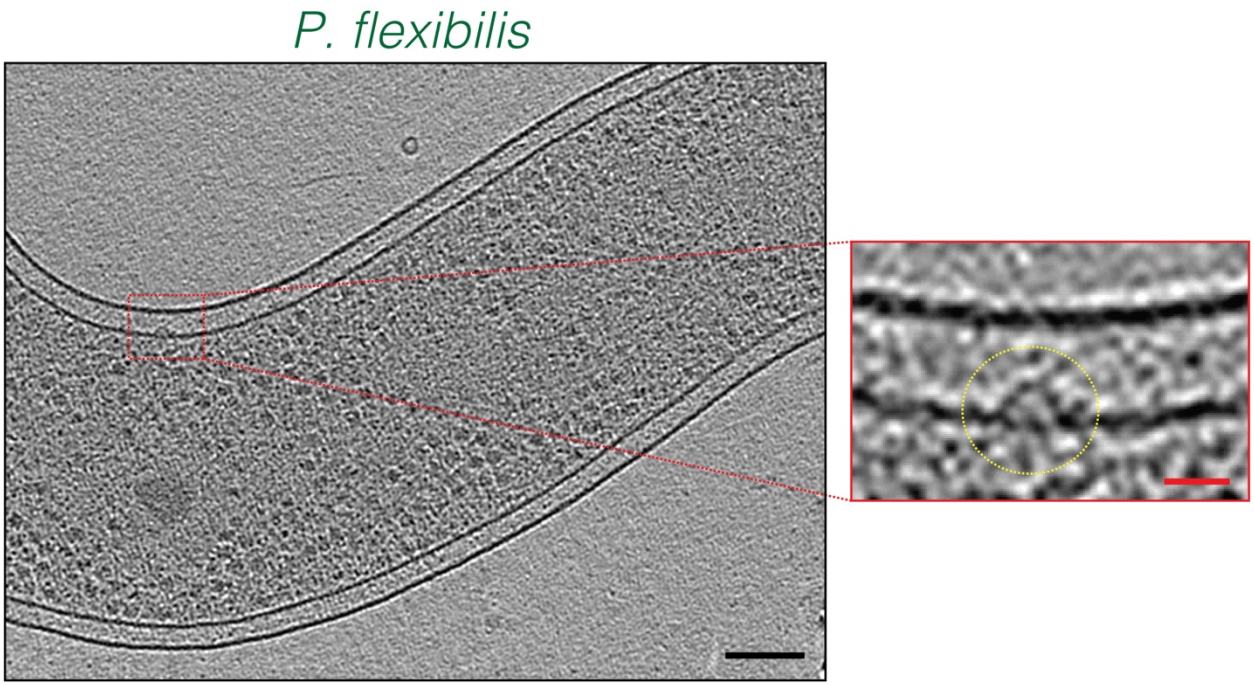

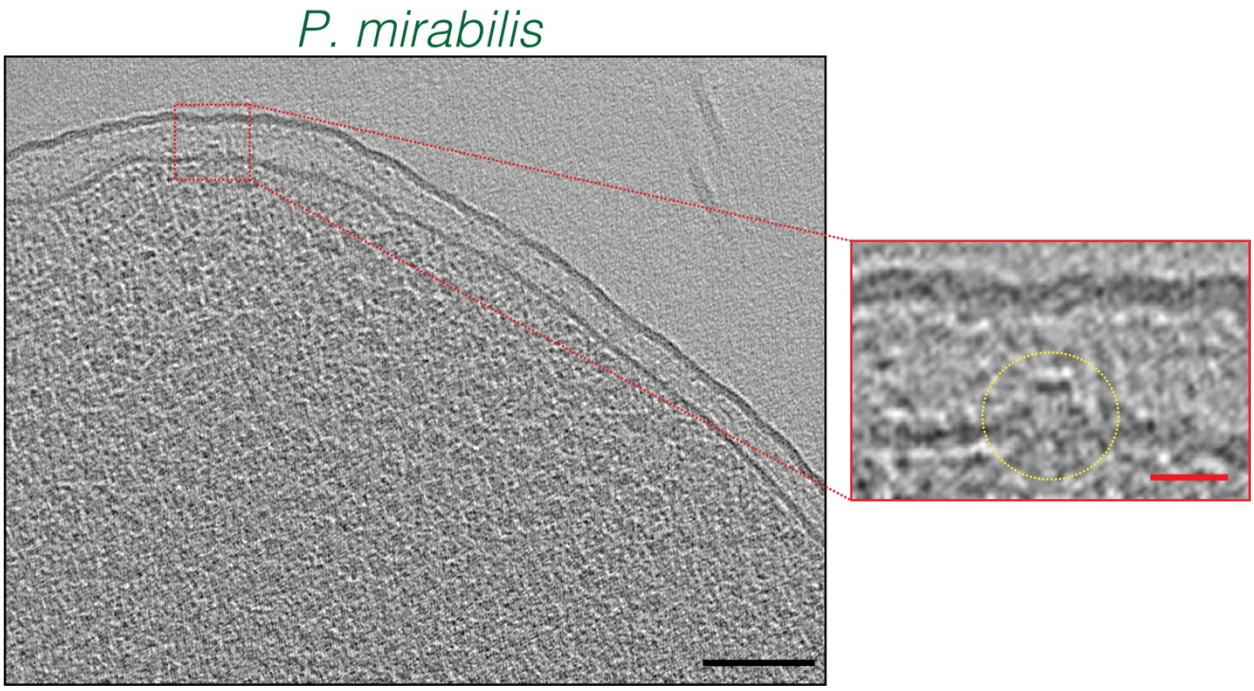

246

247

248

249

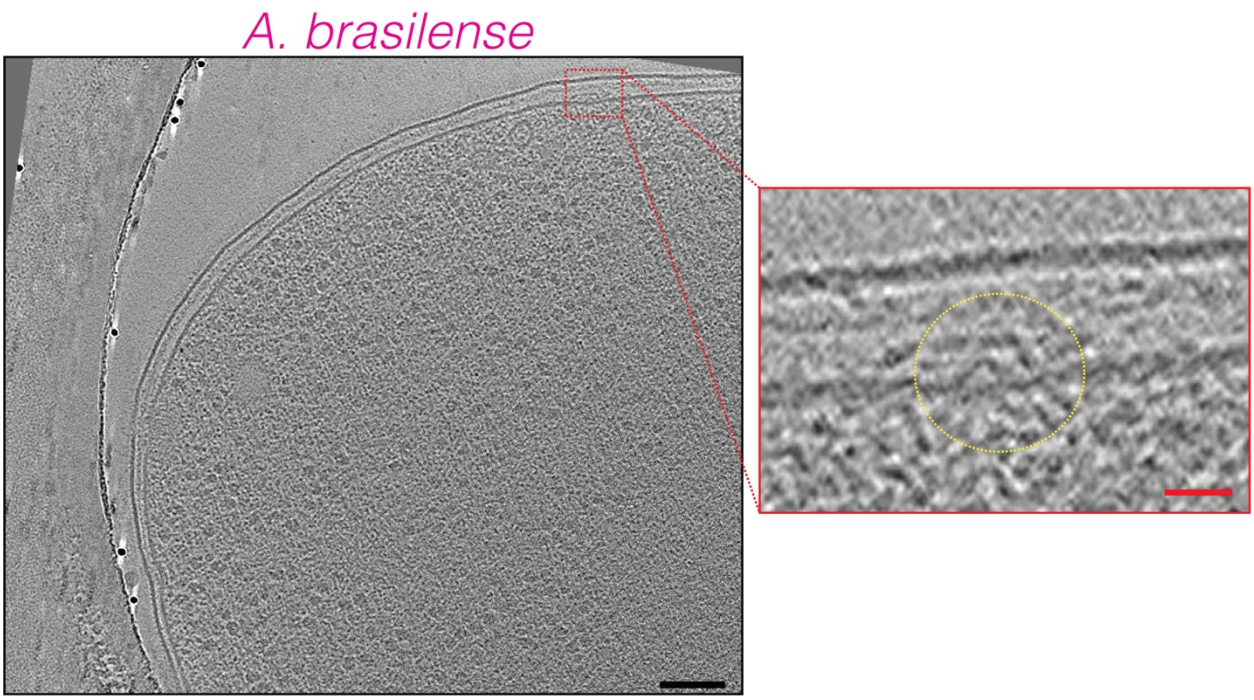

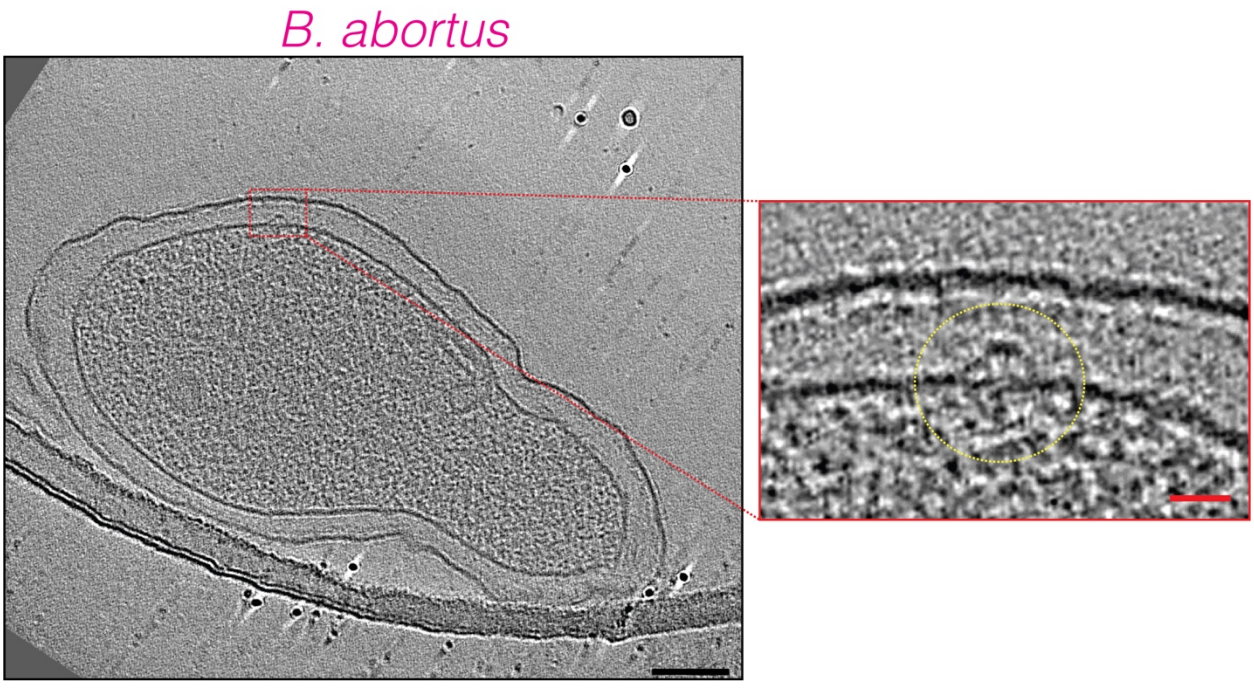

250

251

252

A. tumefaciens

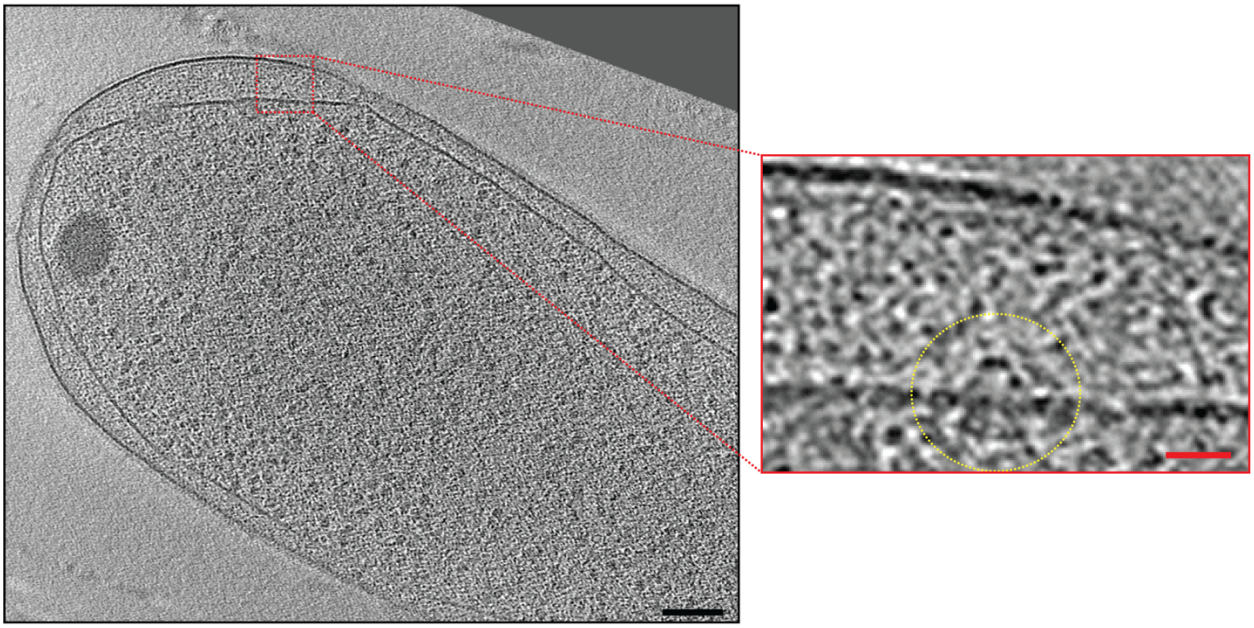

H. neptunium

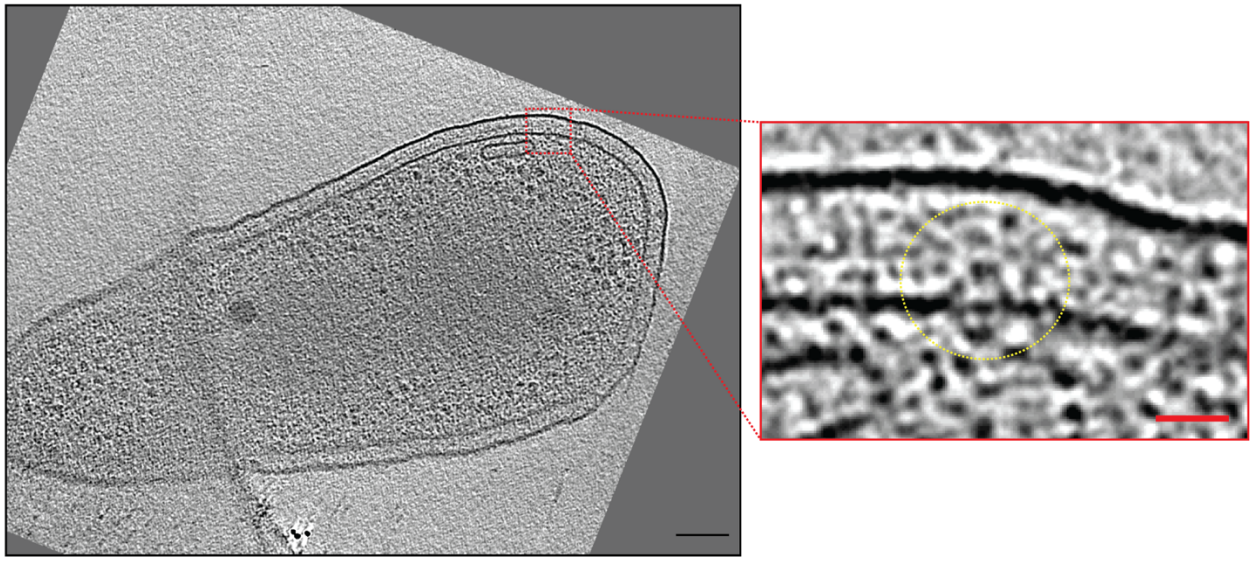

253

254

255

256

257

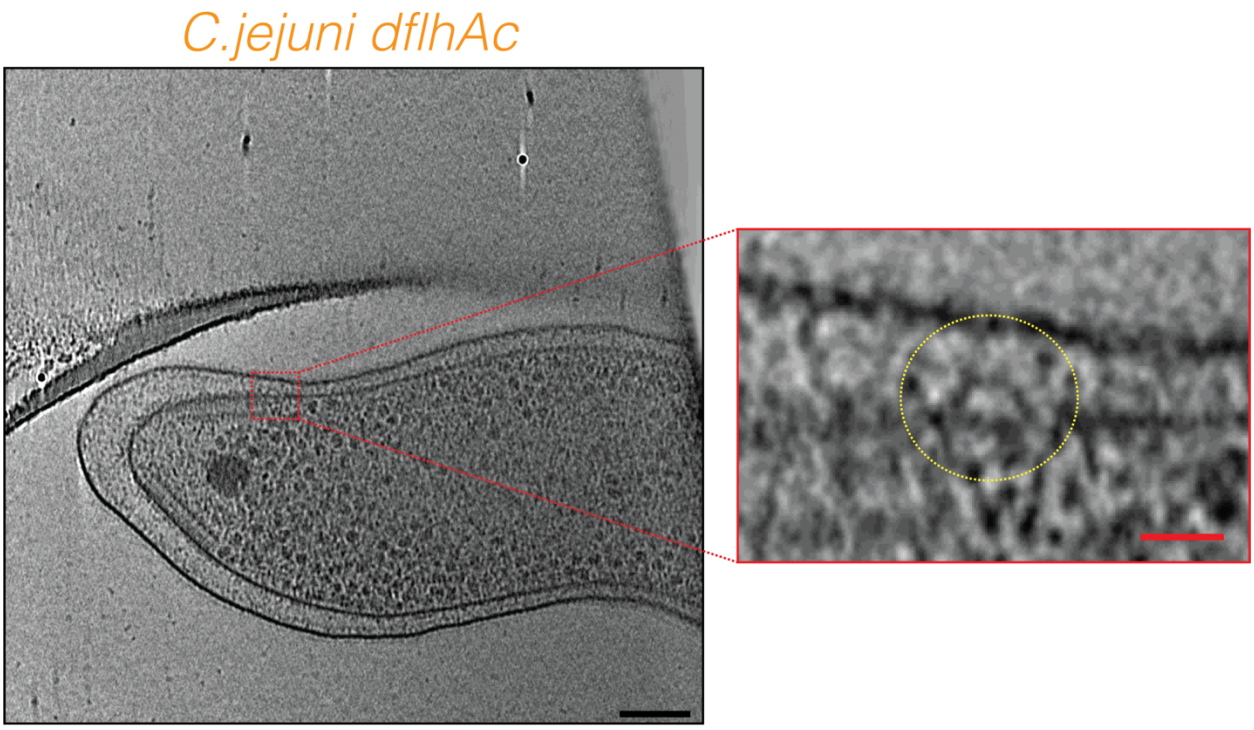

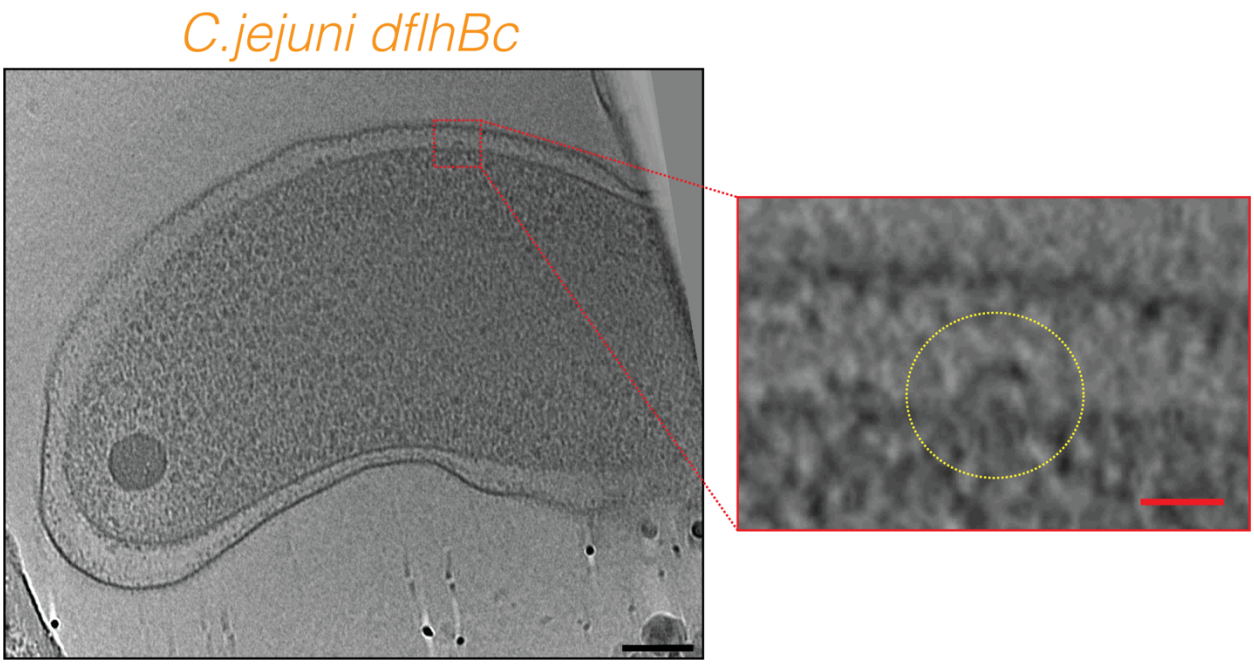

258

259

260

261

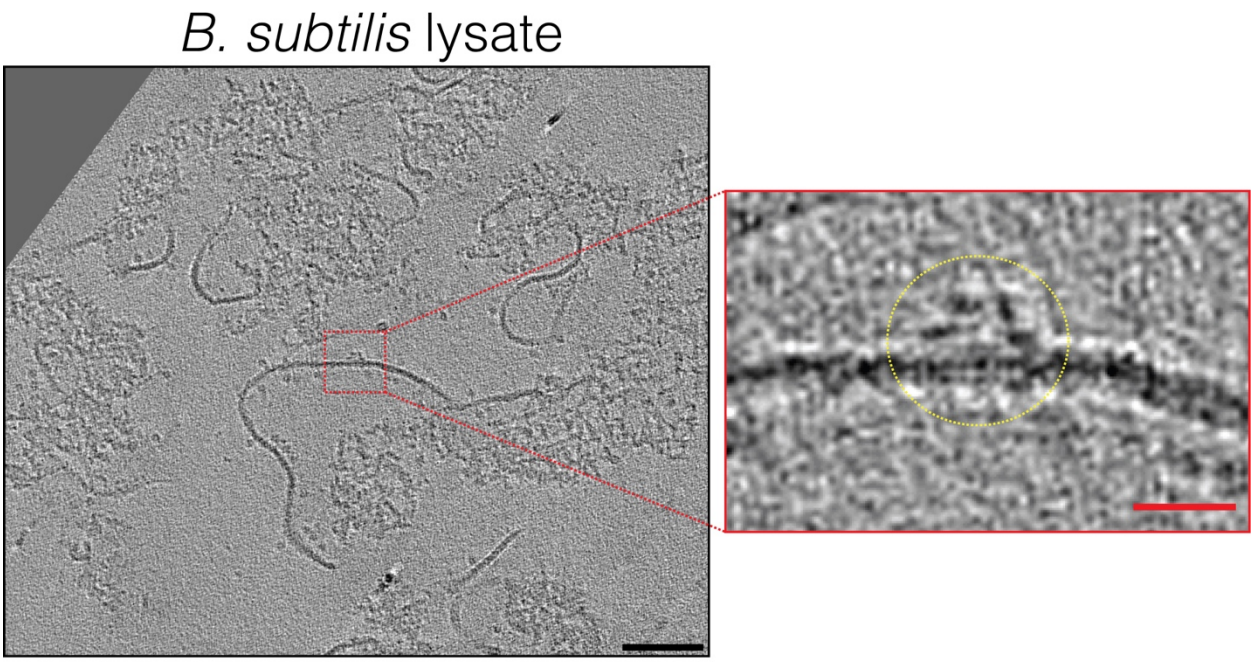

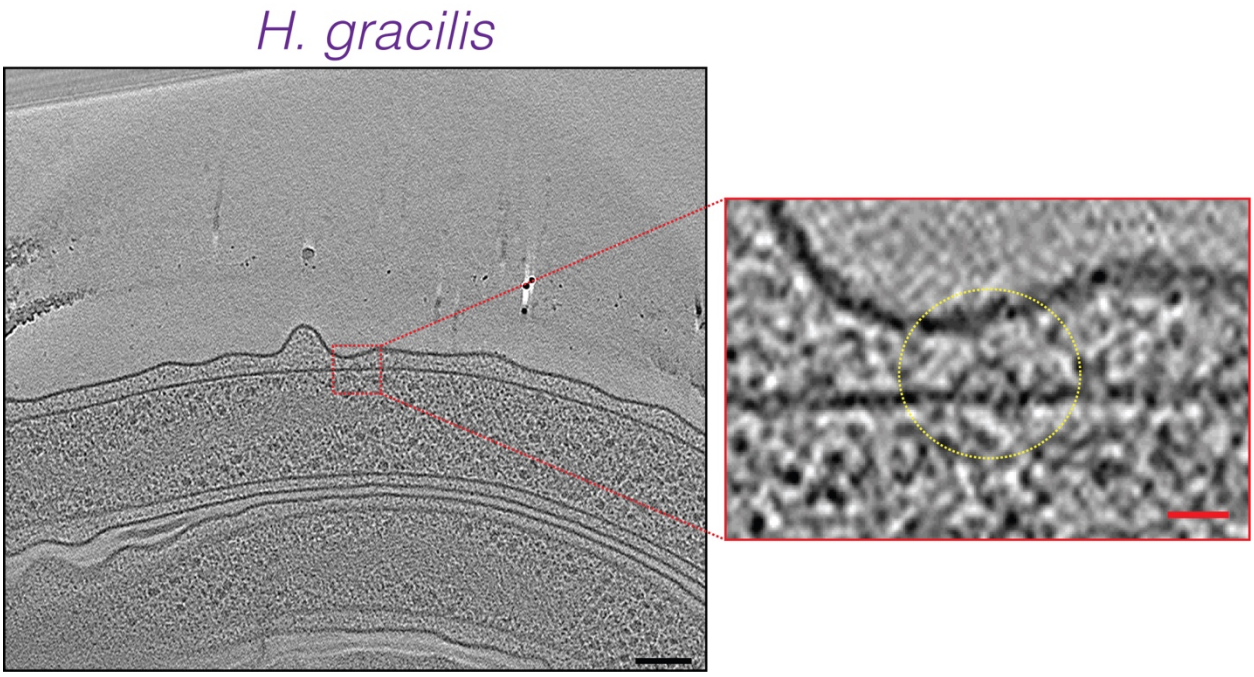

262

263

264

265

Figure S1: Slices through electron cryotomograms of various bacterial species highlighting the presence of hat-like complexes (dotted yellow circles in the enlarged views). Black scale bars 100 nm, red scale bars 20 nm.

Movie S1:

An electron cryotomogram of a partially-lysed *E. coli* cell highlighting the presence of multiple hat-like complexes in the inner membrane (indicated by red circles).

Extended Materials and Methods:

Strains and growth conditions:

E. coli cells were grown as described in ref. [1]. *X. citri* cells were grown in 2xTY medium for 14 hours to stationary phase. *V. cholerae*, *V. harveyi* and *V. fischeri* were grown as previously described [2]. *P. luteoviolacea* were grown as described in ref. [3]. *P. mirabilis* were grown as described in ref. [4]. *P. aeruginosa* were grown in LB medium at 37° C overnight. The *P. aeruginosa flhA** mutant was obtained from a transposon library (mutant number 3296 from the non-redundant library http://pa14.mgh.harvard.edu/cgi-bin/pa14/downloads.cgi) from Dianne Newman's lab at Caltech. *L. pneumophila* were grown as described in ref. [5]. *S. enterica* were grown as in ref. [6]. *P. flexibilis* were grown in Lactose growth medium. *H. neptunium* were grown to exponential phase in PYE medium. *A. tumefaciens* wild-type cells with plasmid-borne VirC1-GFP translational fusion under control of the VirB promoter were grown in AB medium with 150-300 ug/ml of kanamycin. *A. brasilense* and *B. abortus* were grown as described in ref. [7]. *H. hepaticus* ATCC 51449 and *H gracilis* were grown as described in ref. [1,8] *C. jejuni* and its mutants were grown as described in ref. [6,9,10]. *B. subtilis* protoplasts were prepared using lysozyme using a protocol based on ref. [11]. A motile revertant *H. pylori* 26695 isolate was selected by serial passage in Brucella broth supplemented with 10% heat inactivated fetal bovine serum at 37° C, 5% CO_2 for 4 days until cultures reached an OD_{600} ~ 0.4. Non-motile *H. pylori fliP** mutants were propagated on TSAII blood agar plates (BD Biosciences) at 37 °C, 5% CO_2 for either 24 or 48 h prior to collection with a sterile cotton swab for grid preparation. *Helicobacter pylori* mutants (Δ*fliM fliP**, Δ*fliO fliP**, Δ*flgS fliP**, Δ*fliG fliP**, Δ*fliQ fliP**) were grown directly from glycerol stocks on sheep blood agar at 37 °C with 5% CO_2 for 48 hours. Then, the cells were either collected from the plate using a cotton swab and dissolved in PBS and spun down and

plunge-frozen directly, or the cells were spread on a new plate and allowed to grow for 24 hours under the same conditions before plunge-freezing. No difference could be discerned between the two samples by cryo-ET.

H. pylori mutagenesis:

Flagellar mutants were generated in the non-motile *H. pylori* 26695 background as previously described [12]. Briefly, constructs were generated to replace the coding region of the gene of interest with an in-frame, non-polar kanamycin resistance cassette. The target gene and approximately 500 base pairs (bp) upstream and downstream of flanking regions were amplified and cloned into pGEM T-Easy (Promega). This construct was used as a template for inverse PCR to remove the majority of the target gene coding region and to introduce incompatible restriction sites for directional cloning. A kanamycin resistance cassette driven by a promoter transcribed in the same direction as the endogenous operon was cloned into the ligated inverse PCR plasmid. *H. pylori* 26695 was transformed via natural competence, and single colonies resistant to kanamycin (12.5 μg/ml) were selected. PCR was used to verify that the kanamycin resistance cassette had inserted into the target locus in the same orientation as operon transcription.

Electron cryo-tomography sample preparation and imaging:

Sample preparation for cryo-ET imaging was done as described in references [2,13,14]. Total cumulative electron dose used for each tilt-series in each species was:

Species name	Class	Cumulative electron dose (e^-/ Å^2)
Xanthomonas citri	Gammaproteobacteria	120

Vibrio harveyi	Gammaproteobacteria	160
Vibrio fischeri	Gammaproteobacteria	150
Vibrio cholerae	Gammaproteobacteria	160
Salmonella enterica	Gammaproteobacteria	200
Pseudoalteromonas luteoviolacea	Gammaproteobacteria	180
Proteus mirabilis	Gammaproteobacteria	160
Pseudomonas flexibilis	Gammaproteobacteria	100
Pseudomonas fluorescens	Gammaproteobacteria	200
Pseudomonas aeruginosa	Gammaproteobacteria	170
Legionella pneumophila	Gammaproteobacteria	100
Escherichia coli	Gammaproteobacteria	130
Shewanella oneidensis MR1	Gammaproteobacteria	150
Hyphomonas neptunium	Alphaproteobacteria	180
Agrobacterium tumefaciens	Alphaproteobacteria	200
Azospirillum brasilense	Alphaproteobacteria	200
Brucella abortus	Alphaproteobacteria	160
Helicobacter hepaticus	Epsilonproteobacteria	200
Helicobacter pylori	Epsilonproteobacteria	120-130
Campylobacter jejuni	Epsilonproteobacteria	200
Hylemonella gracilis	Betaproteobacteria	75
Bacillus subtilis	Bacilli	160

355

Image processing and subtomogram averaging:

Three-dimensional reconstructions of tilt-series were performed either automatically through the RAPTOR pipeline used in the Jensen lab [15] or with the IMOD software package [16]. Subtomogram averaging was done using the PEET program [17] with a 2-fold symmetrization applied along the particle Y-axis. The number of particles that were averaged are:

Figure	Number of particles
Figure 2 *X. citri*	21
Figure 2 *V. harveyi*	46
Figure 2 *V. fischeri*	19
Figure 2 *V. cholerae*	58
Figure 2 *S. enterica*	38
Figure 2 *P. luteoviolacea*	50
Figure 2 *P. mirabilis*	18
Figure 2 *P. flexibilis*	23
Figure 2 *P. aeruginosa*	78
Figure 2 *L. pneumophila*	149
Figure 2 *E. coli*	31
Figure 2 *H. neptunium*	23
Figure 2 *A. tumefaciens*	29
Figure 2 *A. brasilense*	20
Figure 2 *B. abortus*	41
Figure 2 *H. pylori*	26

Figure 2 *H. gracilis*	30
Figure 2 *B. subtilis*	30
Figure 3A	26
Figure 3B	118
Figure 3C	60
Figure 3D	29
Figure 3E	27
Figure 3F	50
Figure 3G	42
Figure 3H	146
Figure 3J	36
Figure 3K	37
Figure 3L	78
Figure 3M	17

362

363

Supplemental References:

1. Chen S, Beeby M, Murphy GE, Leadbetter JR, Hendrixson DR, Briegel A, et al. Structural diversity of bacterial flagellar motors: Structural diversity of bacterial flagellar motors. The EMBO Journal. 2011;30: 2972–2981. doi:10.1038/emboj.2011.186

2. Kaplan M, Sweredoski MJ, Rodrigues JPGLM, Tocheva EI, Chang Y-W, Ortega DR, et al. Bacterial flagellar motor PL-ring disassembly subcomplexes are widespread and ancient. Proceedings of the National Academy of Sciences. 2020; 201916935. doi:10.1073/pnas.1916935117

3. Shikuma NJ, Pilhofer M, Weiss GL, Hadfield MG, Jensen GJ, Newman DK. Marine Tubeworm Metamorphosis Induced by Arrays of Bacterial Phage Tail-Like Structures. Science. 2014;343: 529–533. doi:10.1126/science.1246794

4. Yao Q, Jewett AI, Chang Y, Oikonomou CM, Beeby M, Iancu CV, et al. Short FtsZ filaments can drive asymmetric cell envelope constriction at the onset of bacterial cytokinesis. The EMBO Journal. 2017;36: 1577–1589. doi:10.15252/embj.201696235

5. Ghosal D, Kim KW, Zheng H, Kaplan M, Truchan HK, Lopez AE, et al. In vivo structure of the Legionella type II secretion system by electron cryotomography. Nature Microbiology. 2019 [cited 22 Nov 2019]. doi:10.1038/s41564-019-0603-6

6. Beeby M, Ribardo DA, Brennan CA, Ruby EG, Jensen GJ, Hendrixson DR. Diverse high-torque bacterial flagellar motors assemble wider stator rings using a conserved protein scaffold. Proceedings of the National Academy of Sciences. 2016;113: E1917–E1926. doi:10.1073/pnas.1518952113

7. Dobro MJ, Oikonomou CM, Piper A, Cohen J, Guo K, Jensen T, et al. Uncharacterized Bacterial Structures Revealed by Electron Cryotomography. Silhavy TJ, editor. Journal of Bacteriology. 2017;199. doi:10.1128/JB.00100-17

8. Briegel A, Ortega DR, Tocheva EI, Wuichet K, Li Z, Chen S, et al. Universal architecture of bacterial chemoreceptor arrays. Proceedings of the National Academy of Sciences. 2009;106: 17181–17186. doi:10.1073/pnas.0905181106

9. Abrusci P, Vergara-Irigaray M, Johnson S, Beeby MD, Hendrixson DR, Roversi P, et al. Architecture of the major component of the type III secretion system export apparatus. Nature Structural & Molecular Biology. 2013;20: 99–104. doi:10.1038/nsmb.2452

10. Müller A, Beeby M, McDowall AW, Chow J, Jensen GJ, Clemons WM. Ultrastructure and complex polar architecture of the human pathogen *Campylobacter jejuni*. MicrobiologyOpen. 2014;3: 702–710. doi:10.1002/mbo3.200

11. DeCastro-Costa MR, Landman OE. Inhibitory protein controls the reversion of protoplasts and L forms of Bacillus subtilis to the walled state. J Bacteriol. 1977;129: 678–689. doi:10.1128/JB.129.2.678-689.1977

12. Shaffer CL, Gaddy JA, Loh JT, Johnson EM, Hill S, Hennig EE, et al. Helicobacter pylori Exploits a Unique Repertoire of Type IV Secretion System Components for Pilus Assembly at the Bacteria-Host Cell Interface. Salama N, editor. PLoS Pathogens. 2011;7: e1002237. doi:10.1371/journal.ppat.1002237

13. Kaplan M, Subramanian P, Ghosal D, Oikonomou CM, Pirbadian S, Starwalt-Lee R, et al. *In situ* imaging of the bacterial flagellar motor disassembly and assembly processes. The EMBO Journal. 2019; e100957. doi:10.15252/embj.2018100957

14. Kaplan M, Ghosal D, Subramanian P, Oikonomou CM, Kjaer A, Pirbadian S, et al. The presence and absence of periplasmic rings in bacterial flagellar motors correlates with stator type. eLife. 2019;8. doi:10.7554/eLife.43487

15. Ding HJ, Oikonomou CM, Jensen GJ. The Caltech Tomography Database and Automatic Processing Pipeline. Journal of Structural Biology. 2015;192: 279–286. doi:10.1016/j.jsb.2015.06.016

16. Kremer JR, Mastronarde DN, McIntosh JR. Computer visualization of three-dimensional image data using IMOD. J Struct Biol. 1996;116: 71–76. doi:10.1006/jsbi.1996.0013

17. Nicastro D. The Molecular Architecture of Axonemes Revealed by Cryoelectron Tomography. Science. 2006;313: 944–948. doi:10.1126/science.1128618

Acknowledgements

This project was funded by the NIH (grant R01 AI127401 to G.J.J., and P20 GM130456 and P30 GM110787 to C.L.S.) and a Baxter postdoctoral fellowship from Caltech to M.K. Cryo-ET work was done in the Beckman Institute Resource Center for Transmission Electron Microscopy at the California Institute of Technology. We are grateful to Prof. Marc Erhardt (Humboldt-Universität zu Berlin) for critically reading an initial version of this work. We thank Prof. Elitza I. Tocheva for collecting the *A. tumefaciens* data, Dr. Jian Shi for collecting the *H. neptunium* data, and Prof. Martin Pilhofer for collecting the *P. luteoviolacea* data.